Princeton Plasma Physics Laboratory

PPPL- 5055

PPPL-5055

Understanding Irreversible Degradation of Nb_3Sn Wires with Fundamental Fracture Mechanics

Yuhu Zhai, Ciro Calzolaio, and Carmine Senatore

AUGUST 2014

PPPL PRINCETON PLASMA PHYSICS LABORATORY

Prepared for the U.S. Department of Energy under Contract DE-AC02-09CH11466.

Princeton Plasma Physics Laboratory
Report Disclaimers

Full Legal Disclaimer

Trademark Disclaimer

PPPL Report Availability

Princeton Plasma Physics Laboratory:

http://www.pppl.gov/techreports.cfm

Office of Scientific and Technical Information (OSTI):

http://www.osti.gov/scitech/

Related Links:

U.S. Department of Energy

Office of Scientific and Technical Information

Understanding Irreversible Degradation of Nb_3Sn Wires with Fundamental Fracture Mechanics

Yuhu Zhai, Ciro Calzolaio, and Carmine Senatore

Abstract—**Irreversible performance degradation of advanced Nb_3Sn superconducting wires subjected to transverse or axial mechanical loading is a critical issue for the design of large-scale fusion and accelerator magnets such as ITER and LHC. Recent SULTAN tests indicate that most cable-in-conduit conductors for ITER coils made of Nb_3Sn wires processed by various fabrication techniques show similar performance degradation under cyclic loading. The irreversible degradation due to filament fracture and local strain accumulation in Nb_3Sn wires cannot be described by the existing strand scaling law. Fracture mechanics modeling combined with X-ray diffraction imaging of filament micro-crack formation inside the wires under mechanical loading may reveal exciting insights to the wire degradation mechanisms. We apply fundamental fracture mechanics with a singularity approach to study influence of wire filament microstructure of initial void size and distribution to local stress concentration and potential crack propagation. We report impact of the scale and density of the void structure on stress concentration in the composite wire materials for crack initiation. This initial defects result in an irreversible degradation of the critical current beyond certain applied stress. We also discuss options to minimize stress concentration in the design of the material microstructure for enhanced wire performance for future applications.**

Index Terms—**Niobium-tin superconducting wires, filament fracture, performance degradation, finite element analysis, fracture mechanics.**

I. Introduction

UNDERSTANDING IRREVERSIBLE performance degradation of advanced Nb_3Sn superconducting wires under mechanical loading is a critical issue for the design of large-scale fusion and accelerator magnets. Recent tests indicate that most ITER cable-in-conduit conductors made of Nb_3Sn wires processed by various fabrication techniques show similar irreversible degradation under cyclic mechanical loading. The irreversible degradation due to filament fracture and strand plastic strain accumulation, however, cannot be described by the existing strand scaling laws. It is important to understand the influence of filament microstructure and initial void distribution on irreversible degradation and irreversible strain limit of Nb_3Sn wires under mechanical loading, and how is the influence correlated with previous microscopic observations of wire filament fracture. These initial voids degrade microstructural homogeneity and may initiate cracks.

Diffusion voids [1] were found to be detrimental to both mechanical and electrical performance of Nb_3Sn wires. These voids are related to the cause of thermal instabilities and crack initiation. There is a trade-off between the increased strain sensitivity and a higher critical current density J_c. On the one hand, increased heat reaction time generates a thicker Nb_3Sn layer and thus a higher J_c. On the other hand, longer reaction time also generates larger diffusion voids and thus increased strain sensitivity. The study of influence of strand geometry on filament fracture in [2] concluded that filament cracking is a result of stress concentration at the voids of bronze wires. Moreover, cracks can propagate across thick Nb_3Sn layer in high J_c internal tin wires. More recently, systematic study of filament fracture distribution in ITER Nb_3Sn strand has been performed independently at University of Twente [3] and Florida State University [4]. Consistent correlations between crack density and the strand electrical irreversible strain limit have been found. The observed high density localized filament fracture for ITER Nb_3Sn CICCs under cyclic loading is a result of large bending under Lorentz force-induced strand movements. Results of previous studies based on post-testing analysis are useful for understanding wire mechanical performance, however, impact of the initial voids during wire fabrication and heat reaction to wire local stress concentration and potential crack initiation cannot be quantified.

Instead of usual post-test examination, in this study, we first carried out the non-destructive X-ray diffraction imaging experiments on various Nb_3Sn wire samples at the Swiss Light Source, PSI, Villigen; we then performed void distribution analysis to extract the voids volume distribution and shape orientation. The void statistical description provides a better understanding of wire mechanics. Finite element models with wire defects were then constructed to study the mechanical response of imperfect wires; and singular elements were implemented into wire models and the fundamental fracture mechanics has been applied to understand impact of defects to the 3-D wire mechanics.

Tomographic imaging experiment combined with fracture mechanics modeling of filament micro-crack formation inside Nb_3Sn wires under increase mechanical loading will improve our understanding to the degradation mechanisms.

Initial voids induced local stress concentration can facilitate crack propagation inside the filament bundle. Linear-elastic fracture mechanics based on stress intensity factor and crack

Automatically generated dates of receipt and acceptance will be placed here; authors do not produce these dates. This work was supported in part by the U.S. Department of Energy under Contract No. DE-AC02-09CH11466. The work was also supported by the University of Geneva-Princeton collaborative Research grants. *(Corresponding author: Yuhu Zhai)*

Y. Zhai is with Princeton Plasma Physics Laboratory, Princeton, NJ 08540 USA, e-mail: yzhai@pppl.gov.

C. Calzolaio and C. Senatore are with the department of Condensed Matter Physics, University of Geneva, Geneva, Switzerland.

tip energy release rate can be used to predict single crack stability and favorable crack growth direction. Correlation with microscopic investigation of filament fracture in terms of crack density, orientation and growth direction will be studied in future work.

II. Experimental Measurement

A. X-Ray Diffraction Tomographic Imaging

A wire measurement campaign was carried out in March 2014 using the TOMCAT beamline of Swiss Light Source at

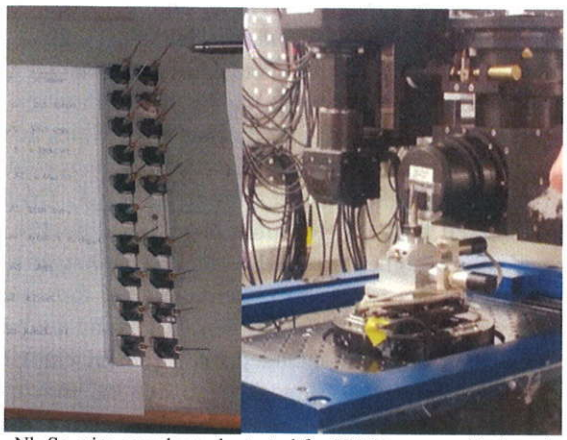

Fig. 1. Nb_3Sn wire samples to be tested for XRD tomographic imaging. The right panel shows the sample holder on the test base rotating 180 degree in horizontal plane during testing to obtain >1200 line-of-sight projections through the wire cross section

the Paul Scherrer Institute, PSI Villigen. X-Ray tomographic imaging of various wire samples has been reconstructed and 2-D images of wire cross-section were processed to extract 3-D void distribution of wires fabricated with the Bronze, internal tin and PIT techniques.

Fig. 1 presents the wire samples to be measured and the sample holder rotated 180 degrees on the test base in the horizontal plane to generate more than 1200 line-of-sight measurements through the wire cross section so images of 2-D slices can be reconstructed.

B. Wire Images with Defects

Defects or initial voids can be formed during the wire fabrication and heat reaction. Fig. 2 presents the 2-D image of

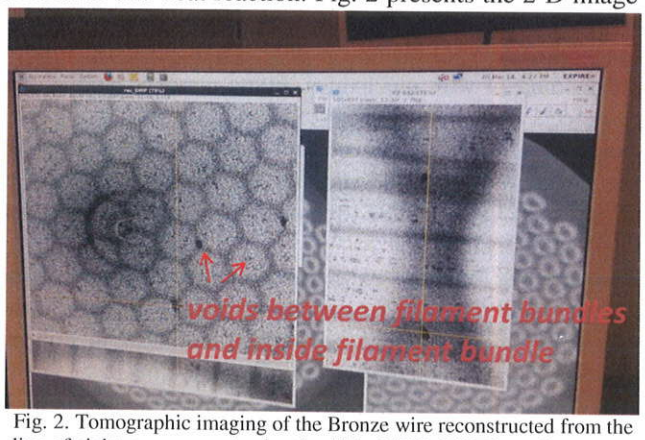

Fig. 2. Tomographic imaging of the Bronze wire reconstructed from the line-of-sight measurement using the 40 keV TOMCAT beamline at PSI.

ITER Bruker Bronze wire tomographically reconstructed. Voids inside and between filament bundles are clearly visible.

C. Three-dimensional Void Distribution

The 3-D microstructure of wire voids can be reconstructed using the 2-D images. Fig. 3 (left) presents the three-dimensional images of voids distribution for the Bruker Bronze wire. A large number of initial voids have been found

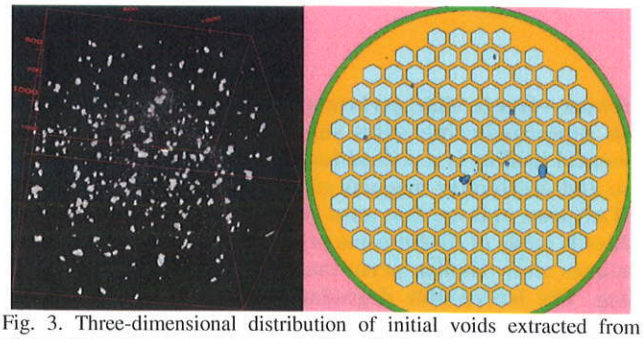

Fig. 3. Three-dimensional distribution of initial voids extracted from slices of two-dimensional images (left) and 2-D projection of 3-D voids in ITER Bruker Bronze wire (right). The voids are located inside the filament bundle and in between filaments.

inside this Bronze wire.

D. 2-D Projected Void Distribution

Fig. 3 also presents 2-D plot of 3-D voids projected onto the cross section of ITER Bruker Bronze wire. Voids of various sizes are clearly seen inside and between the filament bundles. The void information can be implemented into a finite element model of wire composite.

E. Void Distribution Analysis

Detailed void distribution analysis has been performed to obtain the statistical information of void volume distribution, shape orientation and shape descriptor. The statistical description provides better understanding of wire mechanics.

Fig. 4 presents the statistical distribution of void volume

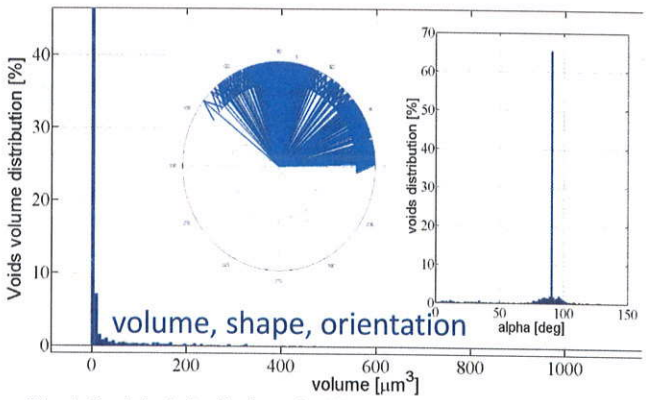

Fig. 4. Statistical distribution of void volume, shape and orientation.

and orientation. Typical size of the voids varies from a few micrometers to a few tens of a micro-meter.

III. Finite Element Modeling

Finite element models of the Bronze wires were developed

based on the ITER Bronze wire geometry. Three-dimensional finite element analysis of Nb_3Sn wire composite with initial voids were then performed. Multi-linear kinematic hardening model described in [5] for Copper, Bronze and Tantalum were used, and linear-elastic Nb_3Sn filament bundle was assumed.

A. 3-D Model of Bronze Wire Composite

The finite element model was validated for cool down of a one millimeter long wire from 923 K reaction temperature to 4 K. The wire has a fixed displacement boundary condition at bottom but no constraint at the top. A 1% total contraction of the wire due to cool down agrees with expected value. The copper and bronze are in tension and Nb_3Sn and Ta are in compression due to thermal mismatch. The 0.15% to 0.2% compressive strain in Nb_3Sn filament bundle is lower than 0.25% expected value since Nb_3Sn is modeled not as small filaments but as sub-element bundle. Fig. 5 presents the axial stress and strain component of the wire top section free of external constraint.

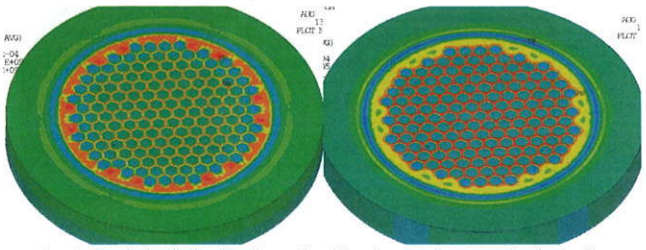

Fig. 5. Statistical distribution of void volume, shape and orientation.

B. Impact of voids to local stress intensity

Two elliptic-shaped initial voids of size 1.5 micrometer by 2.5 micrometer are created inside the wire model. One void has its major axis parallel to the horizontal axis and the other one has its major axis of 45 degree angle with the horizontal axis.

Local stress concentration around initial voids is expected as shown in Fig. 6, where the first principal stress showing local tensile stress concentration around the tip of the voids. The stress intensity factor K_I is 0.5 MPa $m^{0.5}$ at the tip of the horizontal void but increased to 0.7 MPa $m^{0.5}$ for the 45 degree angle void. Existing data of Nb_3Sn fracture toughness [6] showing this brittle material has a fracture toughness of 1.1 MPa $m^{0.5}$.

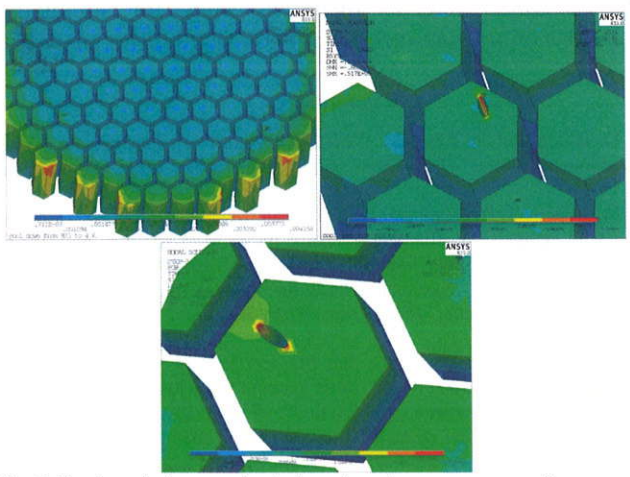

Fig. 6. Total equivalent mechanical strain and stress concentration around the top surface of the two initial voids inside the filament bundle.

IV. Fundamental Fracture Mechanics

A. Linear Elastic Fracture Mechanics

The stress intensity factor and energy release rate [7] can be extracted from the finite element models of imperfect wires. A special singular element has been implemented into the finite element model along the crack front. Since Nb_3Sn filament bundle is assumed to be in a linear elastic region during cool down and axial loading, linear elastic fracture mechanics can be applied.

Two- and three-dimensional fracture mechanics models of wire with embedded voids under a combined compressive and transverse loading have been developed using ANSYS. Fig. 7 presents the stress concentration around crack tip along the local peak tensile stress, where mode I (opening mode) crack growth is likely being initiated.

B. Energy Release Rate and Stress Intensity Factor

For a crack to propagate, the energy release rate will need to be higher than the critical energy release rate, or the stress intensity factor at crack tip shall exceed the crack threshold limit K_{th}. In addition, the rate of the energy release rate along crack front will also need to be greater than or equal to zero. Crack always favors a direction where to lower its total energy state. The energy release rate G is calculated, as in

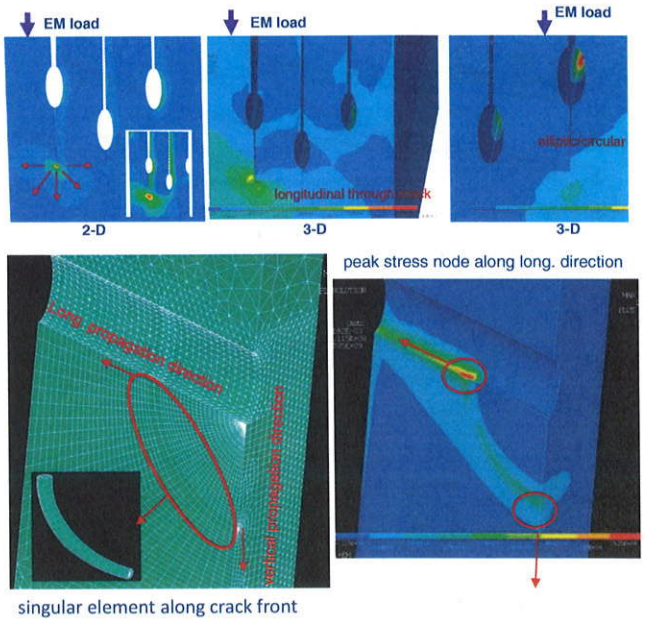

Fig. 7. Crack growth against stress intensity of linear elastic fracture mechanics.

$$G = -\frac{\delta \Pi}{\delta a} = -\frac{\delta (\mathbf{U} + \mathbf{W})}{\delta a} = \frac{1}{2}\mathbf{u}^T \frac{\partial \mathbf{K}}{\partial a}\mathbf{u}. \quad (1)$$

Stress intensity factor around a crack of size a is described

in the following Williams crack tip stress field where y is the crack geometry shape factor,

$$K = \sigma y(a)\sqrt{\pi a}. \quad (2)$$

Crack favors propagation direction that releases more total energy to lower energy state.

C. Micro-crack propagation

Two growth directions have been analyzed as shown in Fig. 7 so to compare the crack tip stress intensity factor extracted following each crack growth step. It is important to know if the crack will propagate longitudinally along the filament bundle or vertically through the filament bundle. If grow vertically, the crack may well be arrested once it reaches the filament-bronze matrix interface due to plastic yielding of

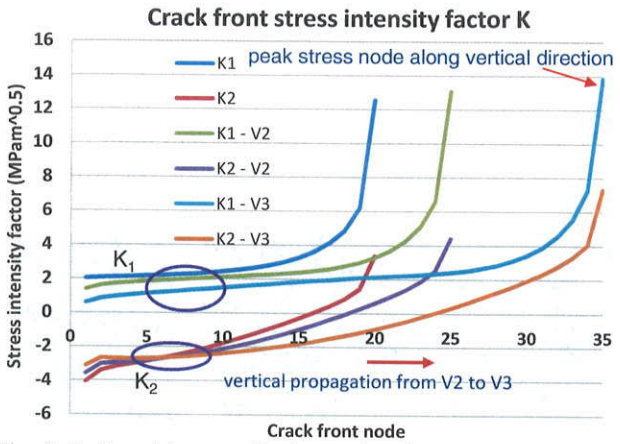

Fig. 8. In item (a), a graphic image that does not meet publication guidelines is displayed.

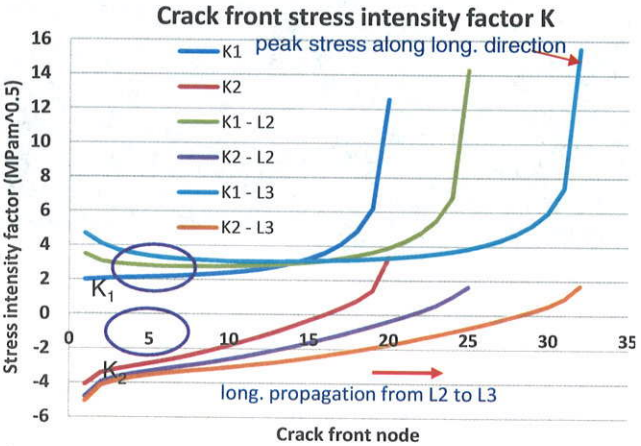

Fig. 9. In item (a), a graphic image that does not meet publication guidelines is displayed.

Bronze.

V. Crack Growth Analysis

The stress intensity factors were extracted from fracture mechanics model analysis where two growth steps are simulated with each step a small growth along the longitudinal direction is assumed while crack front is fixed at the end of the

Vertical propagation	Stress intensity K1 (MPam^0.5)
V0	12.6
V2	13.1
V3	13.9

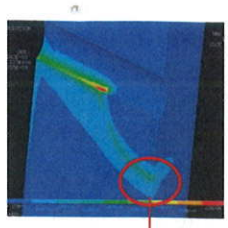

Fig. 10. Stress intensity factor K_I for crack propagates vertically showing lower increase in two growth steps, meaning lower stress state can be reached for crack growing vertically.

longitudinal propagation from L2 to L3

Horizontal propagation	Stress intensity K1 (MPam^0.5)
L0	12.6
L2	14.3
L3	15.5

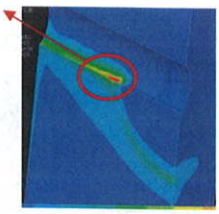

Fig. 11. Stress intensity factor K_I for crack propagates longitudinally showing higher increase in two growth steps, meaning higher stress state for crack growing longitudinally.

vertical direction. Fig. 8 shows plot of the K_I and K_2 factor against crack front node showing in Fig. 7. Likewise, Fig. 9 shows the same plot but assuming crack grows vertically two steps while crack front fixed at the end of the longitudinal direction. The results show a typical mode I opening model crack where $K_I > K_2$.

VI. Conclusion

Fundamental fracture mechanics combined with XRD tomography of Nb_3Sn wires with initial voids can provide new insight to local stress concentration and crack growth within the filament bundles. The approach may also be applicable to HTS such as YBCO and Bi2212 wires since similar wire mechanics and wire composite with defects are expected.

Acknowledgment

Y. Z. would like to thank P. Titus for stimulating discussions on fracture mechanics and crack growth analysis.

References

[1] D. Eason and D. Kroeger, "Kirkendall voids – A detriment to Nb3Sn superconductors," *IEEE Trans. Magn.*, vol. 15, no. 1, pp. 178–181, Jan. 1979.

[2] M. C. Jewell, P. J. Lee and D. C. Larbalestier, "The influence of Nb_3Sn strand geometry on filament breakage under bend strain as revealed by metallography," *Supercond. Sci. Technol.*, vol. 16, 1005, 2003.

[3] A. Nijhuis, et al, "Systematic study on filament fracture distribution in ITER Nb_3Sn strands," *IEEE Trans. Appl. Supercond.* vol. 19, no. 3, Jun. 2009.

[4] A. Nijhuis, et al, "Evidence that filament fracture occurs in an ITER toroidal field conductor after cyclic Lorentz force loading in SULTAN," *Supercond. Sci. Technol.*, vol. 25, no. 7, 075007, 2012.

[5] N. Mitchell, "Finite element simulations of elasto-plastic processes in Nb_3Sn strands," *Cryogenics*, vol. 45, no. 7, pp. 501-515, July, 2005.

[6] M. C. Jewell, "The effect of strand architecture on the fracture propensity of Nb_3Sn composite wires", PhD Thesis, University of Wisconsin-Madison, 2008,

[7] T. L. Anderson, "Fracture Mechanics", 3rd edition, 2004.

Princeton Plasma Physics Laboratory
Office of Reports and Publications

Managed by
Princeton University

under contract with the
U.S. Department of Energy
(DE-AC02-09CH11466)

P.O. Box 451, Princeton, NJ 08543
Phone: 609-243-2245
Fax: 609-243-2751

E-mail: publications@pppl.gov
Website: http://www.pppl.gov